Chapter 8
Modelling Settlement Rank-Size Fluctuations

Enrico R. Crema

8.1 Introduction

This chapter explores the underlying causes of changes in settlement rank-size distribution by modelling the dynamics of group fission and fusion and their responses to different disturbance regimes. The theoretical framework underpinning this exercise is based on the following assumptions:

- The amount of resources at a given location can influence the size of a group located there;
- The relationship between group size and per-capita fitness is expected to increase with increasing group size. Once a critical threshold is exceeded, this relationship is reversed;
- Individuals are expected to improve their condition by means of spatial repositioning, though this will be constrained by limits in knowledge and energy.

An agent-based simulation has been developed in order to establish how variations in the details of these assumptions can induce divergence in the system equilibria, and then to explore how different forms of perturbations (mimicking various forms of endogenous and exogenous environmental deterioration) can alter these.

The chapter will be structured as follows: Sect. 8.2 will provide the background discussion, including an overview on some of the theories underpinning the proposed model; Sect. 8.3 will discuss the details of the agent-based model and how the three assumptions listed above have been formalised. It will also introduce the four different models of disturbance processes examined here; Sect. 8.4 will present the experiment design and the results of the simulation exercise; Finally, Sect. 8.5

E.R. Crema (✉)
University College London, London, UK
e-mail: e.crema@ucl.ac.uk

G. Wurzer et al. (eds.), *Agent-based Modeling and Simulation in Archaeology*,
Advances in Geographic Information Science, DOI 10.1007/978-3-319-00008-4_8

will discuss the wider implications of the model and the main conclusions of the chapter.

8.2 Background

Fission and fusion of human groups can be inferred for a wide variety of temporal scales. Intra-annual events are ethnographically known for many hunter-gatherer groups, who often aggregate temporarily into large groups, only to disperse soon after. For example, the Nootka Indians of the Pacific Northwest coast aggregated into large confederacy sites during the summer while they fissioned into smaller villages during the winter (Drucker 1951, cited in Watanabe 1986). Other ethnographic evidence shows how these fission-fusion cycles can occur with much less regularity and lower temporal frequencies. Historical census data from the Hokkaido Ainu hunter-gatherers provides a good example in this regard. During an interval of 14 years, several sedentary households of the Mitsuishi district fissioned from larger groups or formed new settlements in an irregular fashion (Endo 1995). At a further larger temporal scale, the alternation between dispersion and nucleation of farming communities (Roberts 1996; Jones 2010) have been detected from both historical and archaeological evidence.

Variations in the settlement size distribution are ultimately the result of two processes: the *movements of individuals* and inter-group *differences in the intrinsic growth rate*. The two are related to each other, and in most cases available archaeological evidence is not sufficient to distinguish the outcome of one from the other. However, we can acknowledge their existence if we identify variations in the residential density of a region (a cumulative effect of changes in the overall growth rate) or if we detect the presence of newly formed settlements in a given time window (a direct consequence of fission events).

Despite the difficulty in obtaining direct and reliable proxies of settlement sizes, archaeologists have been long interested in measuring the temporal variation of settlement hierarchy, one of the most tangible consequences of these processes. However, the skewed and long-tailed shape of most settlement size distributions makes the adoption of common statistical measures impractical. Hence, settlement systems are often described using the relationship between rank and size formalised in the following equation (Zipf 1949):

$$S_r = S_1 \cdot r^{-q} \tag{8.1}$$

where S_r is the size of the r ranked settlement, and q is a constant. Equation (8.1) establishes a power-law relationship between size and rank, where the slope is defined by q. When this constant is equal to 1, we obtain the so-called Zipfian distribution, originally considered as equilibrium between "forces of unification" and "forces of diversification" (Zipf 1949).

Fitting equation (8.1) to archaeological data and obtaining empirical estimates of q is a straightforward exercise, and allows us to quantitatively classify different settlement systems. Thus, we can refer to *primate systems* when $q > 1$, that is when we have few large and many smaller settlements. Conversely, when $q < 1$, the system can be classified as *convex*, with the size distribution being more uniform than the Zipfian expectation. However, Drennan and Peterson (2004) noticed that most archaeological data do not appear to conform to such a log-linear relationship between rank and size, and thus devised a more flexible measure explicitly based on the amount of deviation from the theoretical Zipfian distribution ($q = 1$). Their A-coefficient analysis is computed in two steps. First the observed rank-size plot is rescaled, so that the area defined by the end-points of the theoretical Zipf-law distribution is equal to 2. Then the area between the observed and theoretical rank-size distributions is computed, with the area of sections beneath the Zipf's law pattern multiplied by -1. This ensures that the resulting number (the A coefficient) is positive (up to 1) for convex, negative for primate, and close to zero for Zipfian systems. The application of the A-coefficient analysis has increased the number of archaeological cases where the empirical evidence suggests the existence of long-term fluctuations between primate and convex systems (e.g. Drennan and Peterson 2004; Kohler and Varien 2010; Crema 2013a). Several authors have proposed models of generative processes behind these empirically observed rank-size distributions. Hodder (1979) compared the goodness of fit of different stochastic growth models to archaeologically detected rank-size distributions, while more recently Griffin (2011) developed an agent-based model where cycles of consolidation and collapse of complex polities is the primary driver of changes in settlement hierarchy. Others have suggested theoretical linkage between known settlement models and expected deviations from the Zipfian distribution. Thus central place theory, territorial isolation, and low system integration have been linked to convex settlement patterns, while the spatial concentration of resources to the emergence of primate systems (Johnson 1980; Savage 1997).

The two fundamental processes mentioned above (*difference in growth rate* and *movement of individuals*) are still central in these models. Difference in growth rate can be a consequence of variation in resource availability; isolation, low-level integration, and territoriality can be effectively conceived as constraints in the movement of individuals. Here, I consider two sets of theories proposed in behavioural ecology that provide a robust and flexible framework for modelling these two processes.

The first set looks at the attractive and repulsive effect of the external environment, primarily expressed in terms of resource availability. This induced form of spatial dependency (Fortin and Dale 2005), is the central concept of the Ideal Free Distribution (IFD) models (Fretwell and Lucas 1970; Tregenza 1995). The basic prediction in this case is that, given an omniscient population with a complete lack of constraints in movement, the expected population density on a patch will be

proportional to the local resource density. This idea, often referred to as "habitat matching rule" (Fagen 1987), is a consequence of an assumption formally described by the following equation:

$$\phi_i = K_j / n_j \tag{8.2}$$

where the fitness or gain (ϕ) of an individual i at patch j is the ratio between the amount of resource (K) and the number of individuals (n) located there. Thus Eq. (8.2) will be maximised with the lowest population density, and any increase of n will determine a decline in fitness. With other things being equal, individuals will avoid choosing a patch with high resource input if the local population becomes high, and might opt for a patch with lower K as long as n is significantly lower there. This assumption has been further extended, to include the possibility of interference in foraging activities (Sutherland 1983) and the potential to exercise constraints in the movement of other individuals (i.e. ideal despotic distribution; Fretwell and Lucas 1970). Some of these models have also been applied to predict colonisation sequence and settlement history (Kennett et al. 2006; Winterhalder et al. 2010).

One of the key implications of IFD is that aggregation is an indirect consequence of resource distributions. Individuals are "pushed" together, attracted by the presence of richer habitats. Thus a convex settlement pattern should be expected for a landscape with a homogenous distribution of resources while a more primate distribution should result from a heterogeneous setting.

The "push" argument underpinning IFD becomes problematic if one considers the benefits that can potentially derive from aggregation alone. This, in fact, opens to the possibility that individuals might be also "pulled" by the presence of other individuals. Examples of such a positive frequency dependence arising from group formation have been exhaustively discussed in anthropology and ecology, ranging from the benefit of mutual protection (Gould and Yellen 1987) to the possibility of cooperation and more complex organisation of tasks (Hawkes 1992). The presence of these positive frequency dependencies at small population density coupled with negative frequency dependencies at larger sizes is often referred to as the Allee effect in ecology (Allee 1951). The implications of such a non-linear relationship are crucial, and can often lead to unexpected macro-level dynamics. For example, Greene and Stamps (2001) showed how the integration of Allee effect to standard IFD models can lead to the emergence of population clusters that cannot be explained by properties of the resource distribution. Although not explicitly referring to the Allee effect, several authors (Sibly 1983; Clark and Mangel 1986; Giraldeau and Caraco 2000) have also explored the consequences of this non-linear relationship, suggesting, for example, how the expected group size is not necessarily the one in which fitness is maximised (the "optimal group size"), but the one in which this becomes equivalent to the fitness expected by the smallest possible group (the "equilibrium group size").

There are several further assumptions that we need to incorporate in to our model. The foremost is the role of time and, consequently, aspects pertaining inheritance and path dependence in the system of interest (Premo 2010). The Allee effect implies that the attractiveness of a group will dynamically change depending

on the decision of other individuals. Small differences emerging from stochastic components in the system could induce migration flows towards a given group, increasing the fitness of its members, and hence provoking a positive feedback loop. In the long term, however, this process is expected to promote the opposite behaviour, as once optimal group size is reached, fitness will start to decline and individuals will do better leaving the group. As a corollary to this, we also need to consider that fitness will directly affect the long-term behaviour of the system in terms of variation in the intrinsic growth rate.

Similarly, we need to take into account that Eq. (8.2) considers K as parameter constant, and hence invariable over time and by the activities of the local population. The standard IFD model assumes that resources are instantaneously regenerating and hence the abandonment of a patch (and the consequent decline in n) will lead immediately to an increase in the fitness of the individuals who remain there. Externally induced changes in the resource input could tilt the equilibrium of a system, and similarly a reciprocal feedback process between resources and individuals (e.g. K varying over time as a function of n in the past) can lead the system to different equilibria.

Lastly, the level of integration between sub-components of the system (individuals, groups, etc.) should be considered. The non-linear relationship between group size and fitness has been primarily explored without considering the implications of multiple groups co-existing in the landscape. Once we add this to the model (e.g. Greene and Stamps 2001), the dynamics will be partly affected by the level of integration between communities, measurable in terms of physical constraints in the movement (i.e. the cost associated in moving from one place to another, frequency of movement, etc.) and knowledge (i.e. where to go).

8.3 Model Design

We can formalise and extend the three assumptions listed in Sect. 8.1 by generating an agent-based model that embraces the theoretical framework discussed so far.

8.3.1 Basic Model

Consider a population of n agents dispersed in a toroidal landscape composed by P patches. We define a group as a subset of the population of agents located in the same patch. The maximum number of groups will thus be P, and each group j will have a size g_j, defined as the number of agents located in the same patch j. The simulation will proceed through a sequence of discrete time steps $t = 1, 2, 3, \ldots, T$ where the distribution $G_t = g_{j=1}, g_2, g_3, \ldots, g_P$ will be updated by two key processes: *intrinsic population growth/decline* of each group (i.e. reproduction and death), and the *movement of the agents*. Notice that G_t will be essentially equivalent to the

settlement-size distribution at given moment in time t, and hence can be quantified in terms of rank-size. Here, we chose to use the A-coefficient (Drennan and Peterson 2004) described earlier for its flexibility in describing a wider range of patterns. Thus, for each run of the simulation we generate a time series A_t describing the rank-size dynamics of the system.

The core component of the model, which affects both key processes, is the computation of the agent's fitness ϕ. This will be executed in two steps. First the "demand" ξ_i of each agent i will be computed as a random draw from a normal distribution with mean $\mu + (g-1)^b$ and standard deviation ε, where μ is the basic fitness (i.e. the expected yield without cooperation), b is the benefit derived from cooperation, g is the local population density (i.e. the group size), and ε is the stochastic effect of foraging tasks. With other things being equal, ξ_i will increase linearly with increasing group size. The *Allee* effect will be introduced in the second step of the fitness evaluation with the following equation:

$$\phi = \begin{cases} \frac{\sum_i^g \xi_i}{g} & if \ \sum_i^g \xi_i < K \\ \frac{K}{g} & if \ \sum_i^g \xi_i \geq K \end{cases} \tag{8.3}$$

where K is the amount of resource available at the local patch.

The relationship between individual fitness and group size could be potentially modelled in several ways (see Clark and Mangel 1986 for other plausible models), but Eq. (8.3) encapsulates some of the core assumptions regarding human aggregations:

- Grouping provides benefits in the per-capita fitness;
- Some of these benefits will decline in their effect with increasing group size;
- With a further increase in group size, negative and detrimental forces will become predominant, with a resulting decline in the per-capita fitness.

These three points characterise the *Allee* effect described in Sect. 8.2. Here, increasing b will determine a higher average mean per-capita fitness, as long as the total "demand" (sum of all ξ) of the group does not exceed the available amount of resources K. In such a case, the positive effect of cooperation will no longer be sufficient, ultimately leading to a decline in fitness (ϕ).

This non-linear relationship becomes a key element once we explore the two sets of processes that modify group sizes: variation in the intrinsic growth rate and movement of the agents. For the former case, we can translate fitness into a net growth rate, defined as the difference between the probability of reproduction (r) and death (d). We can formalise this as follows:

$$r = \rho \frac{\phi}{\mu} \tag{8.4}$$

$$d = (1 + e^{\phi\omega_1 - \omega_2})^{-1} \tag{8.5}$$

Table 8.1 Fission-fusion conditions and agents' decision-making

Condition 1	Condition 2	Decision
$g_i > 1$ AND $g_w > 1$	$\phi_i \leq \mu - c$ AND $[\phi_w \leq \mu - c$ OR $\phi_i \geq \phi_w]$	Fission
	$\phi_w > \mu - c$ AND $[\phi_i \leq \phi_w - c$ OR $\phi_i \leq \mu - c]$	Migration
$g_i > 1$ AND $g_w = 1$	$\phi_i < \mu - c$ OR $\phi_i < \phi_w - c$	Fission
$g_i = 1$ AND $g_w > 1$	$\phi_i \leq \phi_w - c$	Migration
$g_i = 1$ AND $g_w = 1$	$\phi_i < \mu > \phi_w$	Fission
$g_i > 1$ AND $g_w =$ NULL	$\phi_i \leq \mu - c$	Fission

For all other conditions, the agent stays in the patch where it is currently located; Fission = the agent leaves the group and form a new group with size 1, as long as an empty patch is available within distance h; Migration = the agent joins the group of the model agent w; Fusion = the focal and model agent form a group of size 2

Equation (8.4) establishes a linear increase in the reproductive rate of the agents (controlled by ρ), while Eq. (8.5) has a sigmoidal shape with a small probability of death at high values of ϕ, and an exponential increase of mortality at lower values (cf. Pelletier et al. 1993).

The movement of each agent is assumed to be driven by a mixture of "meliorising" and "satisficing" principles (Mithen 1990), where the key element for evaluation is the "perceived" difference in the observed fitness. The model will produce fission and fusion dynamics based on the following algorithm, triggered with frequency z:

1. A focal agent i defines a pool of observed agents S as a random sample of proportion k of agents located within distance h from i.
2. The agent with the highest fitness among the pool S will be defined as the model agent w. If S is an empty set, there will be no model agent.
3. The focal agent i will compare its own group size (g_i) and fitness (ϕ_i) with: the model agent group size (g_w), the model agent fitness (ϕ_w), and the basic fitness (μ). The comparison will be calibrated by a threshold of evidence c (Henrich 2001), representing the propensity of the agent to be conservative (high c) or not (low c).
4. As a result of this comparison the agent will decide to stay in the current group, join another group, or form a new group on its own (see Table 8.1).

8.3.2 Integrating Disturbance

The model presented so far is primarily defined by parameters that describe the behaviour of the agents. The only exception is the resource input size K, a state variable of the patches where the groups are located, and hence independent to the agents. Thus if we want to explore the intrinsic properties of the system we can assume K as a constant and invariable parameter. This can provide a benchmark model (*scenario 0*), where we can identify the key properties of the system in a

controlled condition where the dynamics are exclusively the consequence of the agents' behaviour. Subsequently, we can relax this assumption, and explore the effects of disturbance, i.e. variation of K, under the following four scenarios.

The first (*scenario 1*) explores the effect of spatial heterogeneity by adding to the initial homogenous distribution of K a random integer with mean 0 and variance v. Increasing values of v will increase the heterogeneity of the resource distribution, maintaining, on average, the total productivity (the sum of all K of all cells) of the system constant. The benchmark model (*scenario 0*) can be regarded as a special case of this scenario where v is equal to 0.

The second scenario (*scenario 2*) will relax the assumption of the temporal homogeneity, allowing K to be time-variant. This will be modelled as a bounded random walk, iterating the same algorithm used for scenario 1 for each time-step in the simulation, again parameterised by v. To avoid excessively high or low values of K, the process will be "bounded" between K_{lo} and K_{hi}. High values of v will generate abrupt shifts, while lower values will lead to gradual changes in the resource availability. The third scenario (*scenario 3*) will combine the assumptions of scenarios 1 and 2, allowing the resource input of each patch to have an independent bounded time-series of K.

In contrast to the models of disturbance proposed so far, the last scenario (*scenario 4*) shapes the spatio-temporal variation of K as a result of a predator-prey relationship with the agents. The assumption in this case is that high local population density should, in the long term, determine a degradation of the local environment and a decline in resource productivity. This differs somewhat from the detrimental role of overexploitation portrayed in Eq. (8.1), as the effect will be also time-dependent (i.e. a group might experience a long-term decline in fitness even if g is hold constant). The predator-prey relationship can be formalised with the following pair of equations:

$$\Xi = \begin{cases} \sum_i^g \xi_i & \text{if } \sum_i^g \xi_i \leq K_{t-1}(1-\beta) \\ K_{t-1}(1-\beta) & \text{if } \sum_i^g \xi_i > K_{t-1}(1-\beta) \end{cases} \tag{8.6}$$

$$K_t = (K_{t-1} - \Xi) + \zeta(K_{t-1} - \Xi)\left(1 - \frac{K_{t-1} - \Xi}{\kappa}\right) \tag{8.7}$$

Equation (8.6) defines the cumulative gain Ξ of the agents—which becomes the individual fitness once its divided by the group size—and is subtracted from the resource input in Eq. (8.7), a variant of the Verhulst equation (Verhulst 1838), defined by an intrinsic growth rate ζ and a carrying capacity κ. Equation (8.7) thus ensures that K is modelled as a population affected by the consumption rate Ξ of the agents. The parameter β in Eq. (8.6) models the resilience of the resource pool: high values will determine an under-consumption of the agents (i.e. the agent will not be able to identify and consume all resources located on a given patch), while low values will increase the likelihood of complete resource depletion.

8.4 Results

The simulation code was written in R statistical computing language (R Core Team 2013) and is available under request. All experiments have been conducted using UCL Legion High Performance Cluster. A wider exploration of the parameter space for the benchmark model (*scenario 0*) is extensively discussed elsewhere (Crema 2014). Here we purposely sweep only the key parameters that have been previously identified as those[1] determining the largest variation in the system behaviour: the spatial range of interaction h; the frequency of decision-making z; and the sample proportion of the observed agents k. We additionally sweep three values for relevant parameters describing different disturbance processes (v for scenarios 1, 2 and 3, and β for scenario 4). In this case, the choice of parameter values has been dictated by preliminary explorations of the model in a simplified environment with a single group (P = 1), where the effect of movement has been excluded. This exercise allowed the detection of a key range of values covering the widest spectrum of behaviours in the simplified model. For example, a small variation of β from 0.3 to 0.4 was sufficient to cover the phase transition between three equilibria in a single group model: extinction (Fig. 8.1a), limit-cycle (Fig. 8.1b), and sustainable population (Fig. 8.1c). Similarly, the values of v for scenarios 2 and 3 were selected by observing the proportion of runs where the single group was extinct after 500 time-steps. This helped providing a rough proxy for defining light ($v = 9$, 0.2 extinction rate), intermediate ($v = 16$, 0.5 extinction rate) and severe ($v = 37$, 0.9 extinction rate) disturbance processes (see Fig. 8.1e).

The resulting parameter space (see Table 8.2) has four dimensions and 34 coordinates. For each unique parameter combination, the simulation has been computed 100 times with 500 time steps each. Given that the primary focus of the simulation is to establish the equilibrium properties of the system, the first 200 time-steps have been discarded from the analysis as a "burn-in" stage.

The results of the simulation exercise can be illustrated using a scatter-plot of A_t against A_{t+1}. This data representation can help identify whether the rank-size pattern is stable (point attractor), oscillates between two extremes (limit cycle attractor) or fluctuates chaotically (strange attractor; see McGlade 1995 for a detailed discussion on attractors and their relevance in archaeology), and shows, at the same time, the observed range of variation as well as the frequency and the magnitude of changes (see Fig. 8.2).

[1]The parameters defining reproduction (ρ), death (ω_1 and ω_2), cooperation (b), and threshold of evidence (c) can be all aggregated into different types of relationship between key group sizes and net-growth rate. Crema (2013b) showed that the dynamics were significantly different only when the net-growth rate was extremely low and equivalent to zero at the equilibrium group size (i.e. the value of g satisfying the conditions $\phi(g) = \phi(1)$ and $g > 1$). The parameter values chosen for this chapter determines a net growth rate which remains positive above this size.

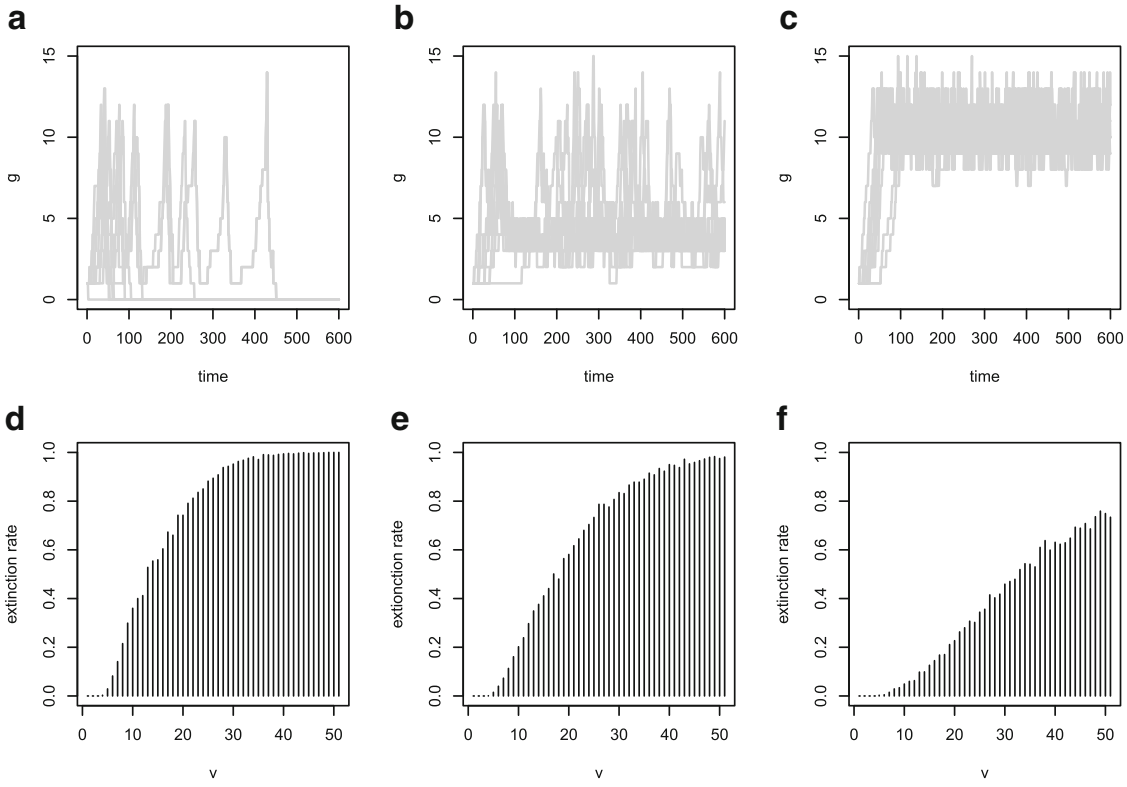

Fig. 8.1 Preliminary exploration of the simulation model. The *upper row* (**a–c**) depicts three sets of ten time-series of population change with the effects of different parameter settings of β ((**a**): $\beta = 0.3$; (**b**): $\beta = 0.35$; (**c**): $\beta = 0.4$). The *lower row* shows the proportion of runs with extinction (among 1,000 simulation runs) for different settings of v and three distinct values of K_{lo} ((**d**): $K_{lo} = 0$; (**e**): $K_{lo} = 10$; (**f**): $K_{lo} = 20$; in all cases K_{hi} was set to 400). In all cases the experiments have been conducted using a single patch world, with the settings listed in Table 8.2

8.4.1 Benchmark Model and Spatial Heterogeneity (Scenarios 0 and 1)

Figure 8.3 shows the parameter space for scenarios 0 and 1. The primary axis of variation in the system behaviour is along an increasing frequency of decision making (z), higher knowledge (k), and wider range of interaction (h), while the effects of increasing heterogeneity of the resource distribution (v) appears to have almost no effect. When z, k, and h have their smallest values, the system is highly disconnected, and the agents distribute themselves to local optima (the best patch around their neighbourhood) leading to the formation of stable convex systems.

The spatial range of interaction plays a pivotal role in this scenario, as increasing values of any of the other three parameters do not affect alone the broad properties of the system (i.e. the type of attractor), expect for larger fluctuations of A around smaller mean values. Once the spatial range of interaction is increased ($h \geq 3$), the implications of the other three parameters become evident in the scatterplots. Agents can now move freely in the landscape and hence the effects of their movement

Table 8.2 List of parameters and values

Symbol	Name	Values
P	Number of patches (cells)	100
μ	Basic fitness	10
b	Benefit of cooperation	0.5
ε	Basic payoff variance	1
ρ	Basic reproductive rate	0.05
ω_1	Death parameter 1	1.2
ω_2	Death parameter 2	5
z	Frequency of decision-making	0.1, 0.5, 1.0
h	Spatial range of interaction	1, 3, 10
k	Sample proportion of observed agents	10^{-8}, 0.5, 1.0
c	Threshold of evidence	3
K	Resource input	200
v_S	Stochastic disturbance parameter (scenario 1)	0, 10, 50
v_T	Stochastic disturbance parameter (scenario 2 and 3)	9, 16, 37
K_{lo}	Lowest possible K	10
K_{hi}	Highest possible K	400
ζ	Intrinsic growth rate of K	2
κ	Carrying capacity of K	200
β	Resource resilience to predation (scenario 4)	0.3, 0.35, 0.4

propagate at larger scales, rather than being absorbed locally. As a consequence of this, we can identify an increase in the possible range of values for A and the occasional appearance of primate systems ($A < 0$). However, in most cases these highly hierarchical settlement systems are unstable, as suggested by the smaller density of points in the lower-left quadrants (see $h \geq 3$, $k \geq 0.5$, $z = 0.5$ in Fig. 8.3).

When the frequency of decision-making is set at its maximum ($z = 1$), the range of spatial interaction is sufficiently high ($h \geq 3$) and the sample proportion of observed agents (k) is equal or larger than 0.5, the system exhibits a limit cycle attractor. The scatterplot also shows how the patterns of these limit cycles are affected by the spatial range of interaction, with $h = 3$ showing more gradual transition between primate and convex pattern, and $h = 100$ characterised by rapid shifts (compare with Fig. 8.2). This cyclical dynamic is derived from the high convergence in the tempo of the decision-making (i.e. all agents move at the same time) and the destination of the migration flow (i.e. all agents move to the same place). Slightly optimal groups are rapidly identified and invaded, triggering a positive feedback, which promotes further migration. This becomes soon unsustainable, and once the destination group becomes too large and fitness starts to decline fission events reset the cycle.

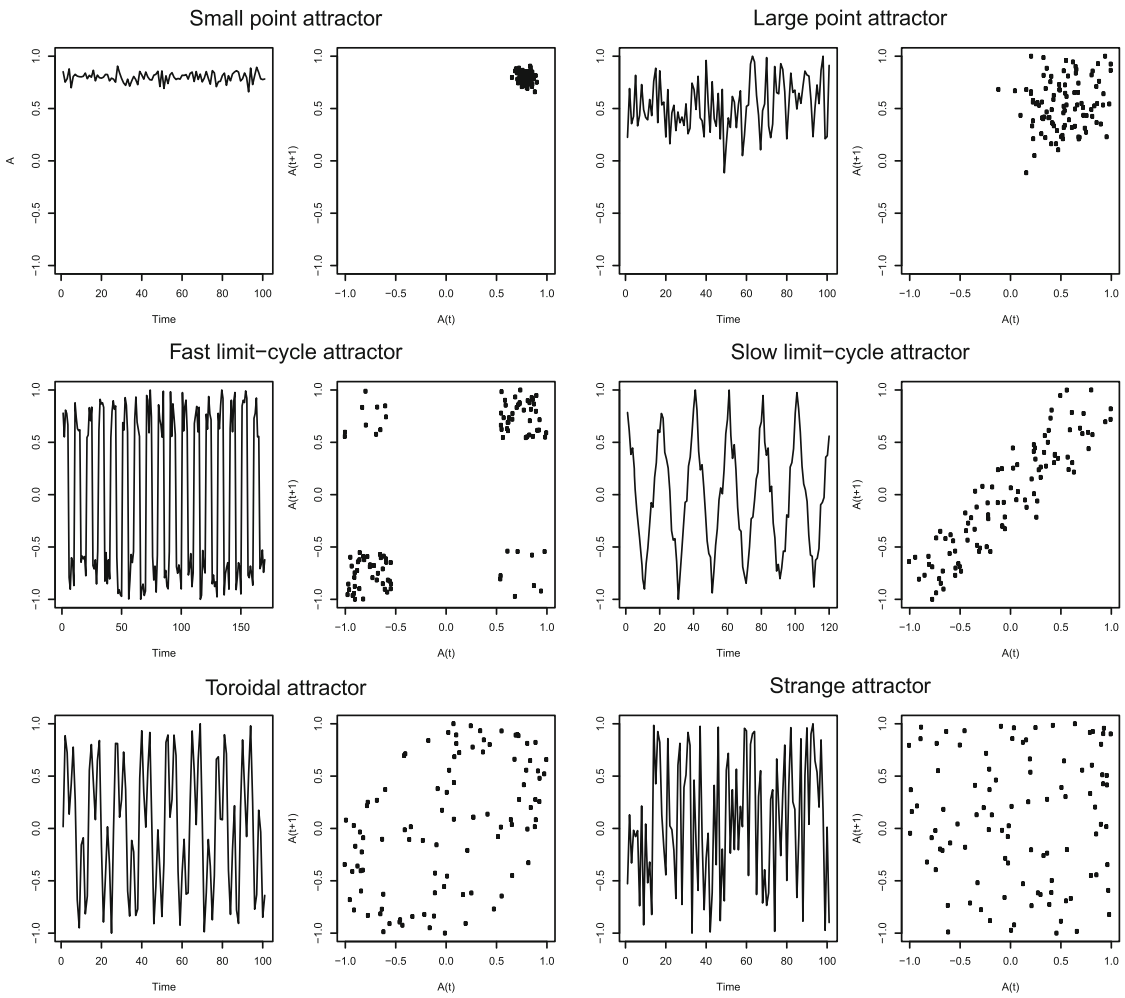

Fig. 8.2 Phase-space scatter plots for different types of time-series (attractors) of A

8.4.2 Temporal and Spatio-Temporal Disturbance (Scenario 2 and Scenario 3)

The pivotal role played by the level of integration between groups is still evident when we add time-varying forms of disturbance processes. Figure 8.4, which depicts the parameter space for scenario 2, shows in fact that low levels of k, z, and h lead to convex point attractors, while their increase determine the emergence of continuous shifts in the rank-size distribution. Details on these shifts are contingent to the time-series of K of individual runs, but we can still identify general trends of regularity (e.g. in $z \geq 0.5$, $k \geq 0.5$, $h \geq 3$), suggested by the higher density of points along the diagonal (see also Fig. 8.2).

When the frequency of decision-making (z) is at its highest value (i.e. the agents respond immediately to the perceived variation in fitness) and the spatial range of interaction (h) is equal or greater than 3, we can observe a limit-cycle attractor with relatively few irregular sudden shifts (lower density of points in the top-left and bottom-right quadrants). However, when $z = 0.5$, the number of unexpected

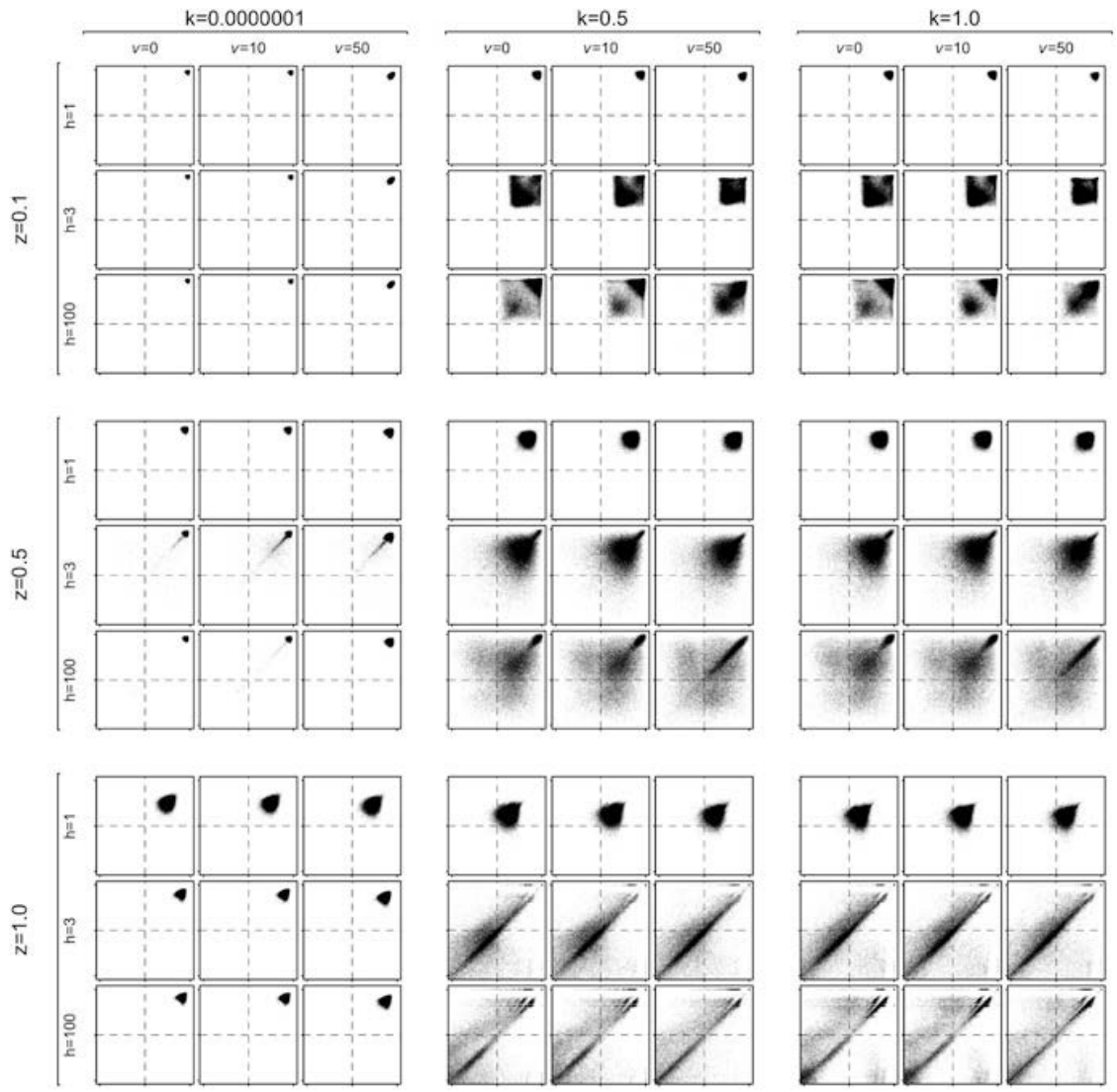

Fig. 8.3 Parameter-space for Scenarios 0 and 1. The x and y axes represent A_t and A_{t+1} and range from -1 to $+1$

changes in the rank-size distribution is much higher, and the system can be classified as a hybrid between limit-cycle and strange attractor. This is most likely explained by a slower response rate of the agents, which are forced to face the consequence of decline (or increase) in K before their relocation. Recall in fact that in the basic, disturbance-free model the system already exhibits high frequency shifts between primate and convex distributions at the highest values of h and z. Hence, within these regions of the parameter space, the disturbance process has a marginal role as the basic dynamics of the system occur at a faster rate. In other words agents relocate themselves before perceiving the consequences of the disturbance events. Conversely, when the response rate is slower ($z = 0.5$), the agents are affected by changes in K. Variations in the abruptness of these disturbance events (v) do not seem to play a significant role other than minor variations in the dispersion of the scatter points: the smallest variation in the availability of resources (K) can be sufficient to induce a cascade effect into the system.

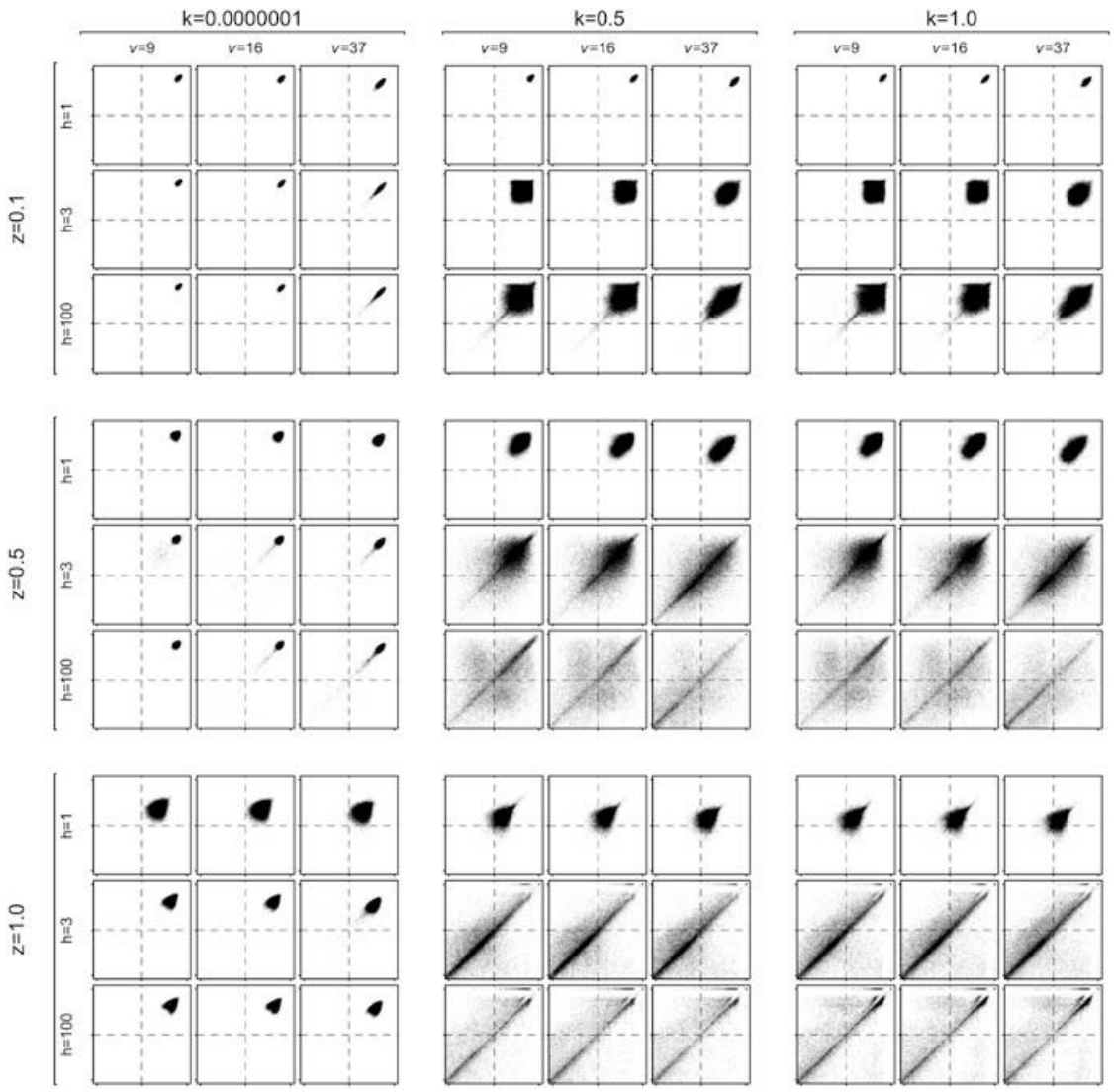

Fig. 8.4 Parameter-space for Scenario 2. The x and y axes represent A_t and A_{t+1} and range from -1 to $+1$

Scenario 3 (Fig. 8.5), which combines both the assumption of spatial heterogeneity and temporal changes of K, shows similar patterns. Once again the largest variation of the phase-space scatter plot can be observed along the axes defined by h, z, and k. This time, however, increasing values of v exhibit a diagonal "tail" in regions of the parameter space that are characterised by point-attractors in the benchmark model. Observation of individual runs indicates that these pattern are generated from the slow recovery of the system towards highly convex distributions after episodes of sudden decline in A caused by disturbance events. As for scenario 2, the effect of disturbance is tangible mostly for intermediate levels of z, where we can observe increasing episodes of deviations from convex systems with larger values of h and a transition from a "noisy" point attractors to a hybrid between limit cycle and strange attractors. When z is at its highest, the frequency of decision-making is higher than the frequency of disturbance events, leading to a general pattern similar to the benchmark model.

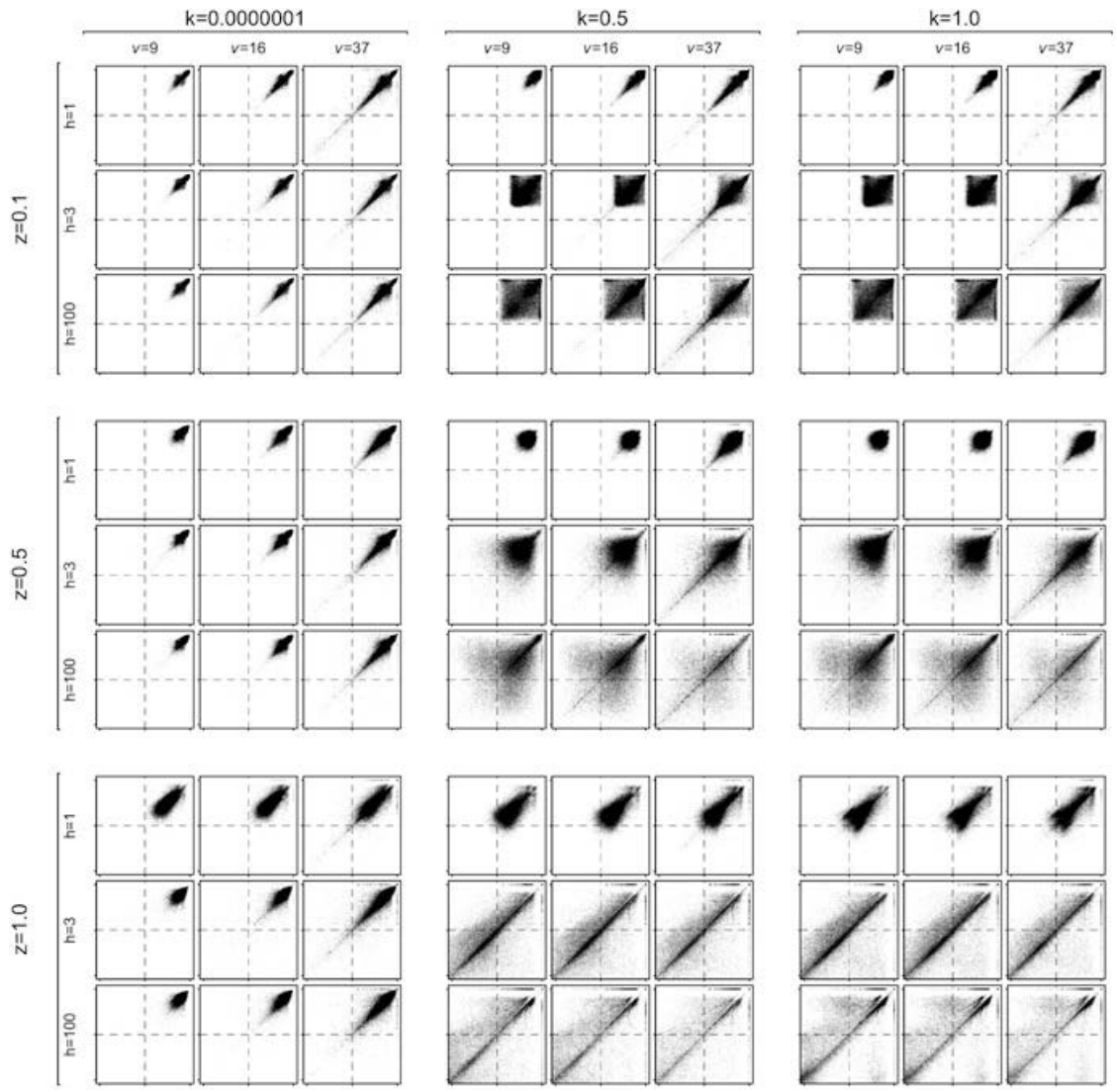

Fig. 8.5 Parameter-space for Scenario 3. The x and y axes represent A_t and A_{t+1} and range from -1 to $+1$

8.4.3 Predator-Prey Model (Scenario 4)

Figure 8.6 illustrates the parameter space for scenario 4, where the amount of resource input K at a given patch is defined by a predator-prey relationship with the group of agents located there. Although this time disturbance can be regarded as endogenous (contra-posed to the exogenous disturbance events of scenarios 1–3), the basic properties of the system remains the same: high levels of h, z, and k still lead to stronger and more frequent variations in the rank size distribution.

The most relevant difference with the other scenarios is how the parameter defining the disturbance process (i.e. the resilience of the resource population β) appears to have a stronger influence in the simulation output. When this is set to the lowest value explored in this series of experiment ($\beta = 0.3$), we observe a larger dispersion of the phase-space scatter plot, often leading to the emergence

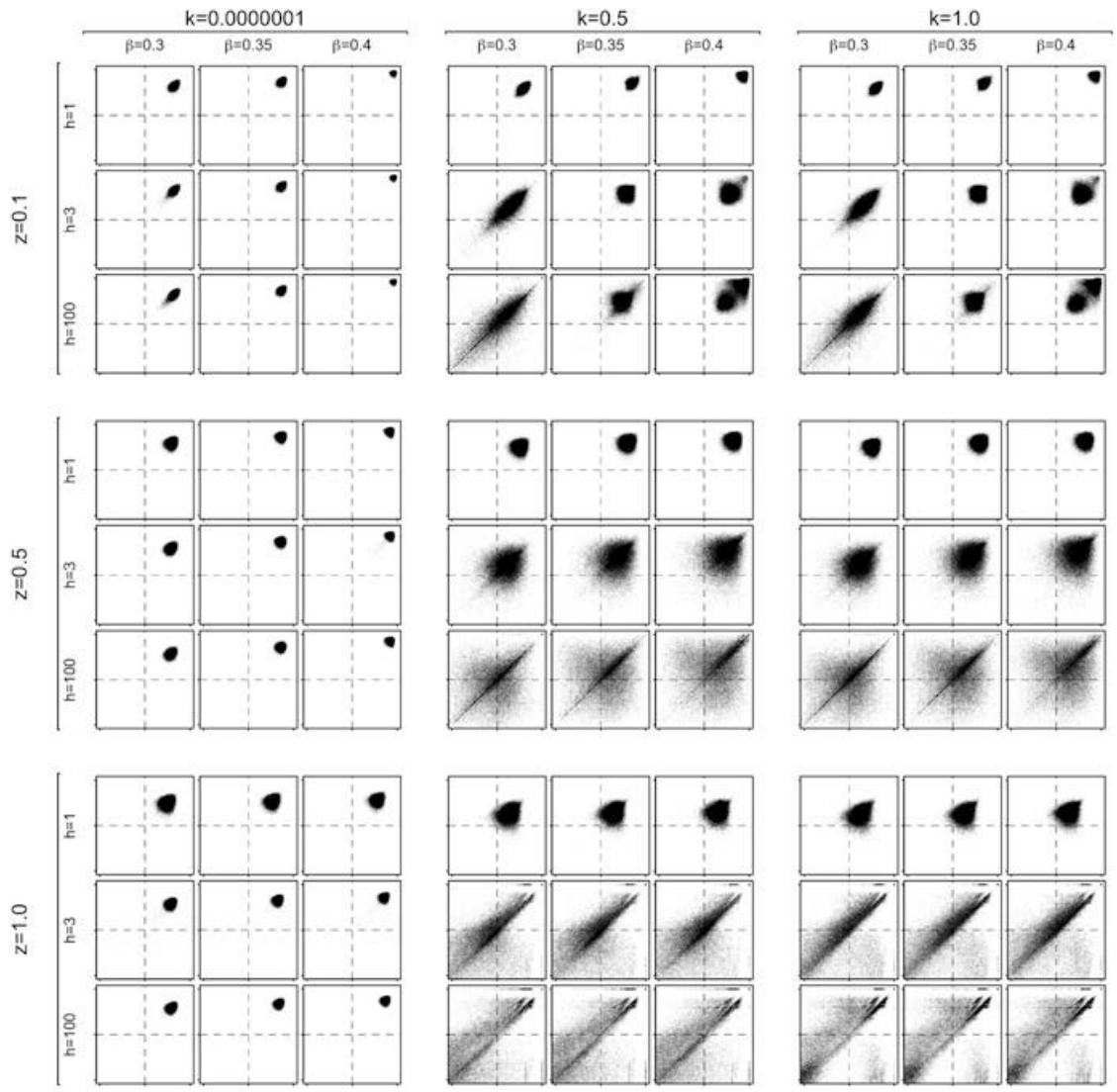

Fig. 8.6 Parameter-space for Scenario 4. The x and y axes represent A_t and A_{t+1} and range from -1 to $+1$

of limit-cycles even when the frequency of decision making is at its lowest. This is the consequence of the ecological inheritance modelled by Eq. (8.7): agents will be subject to a decline in fitness even when there is no internal growth or migration flows. However, if the sample proportion of the observed agents and the spatial range of interaction are also low we still observe exclusively convex point-attractors, confirming once again that the level of integration still plays a pivotal role in explaining the temporal variation in the settlement pattern. When the frequency of decision making is set at its maximum, variations in β do not seem to affect the properties of the system, although the scatter plots appear to be in all cases characterised by a larger number of points outside the main diagonal. As for scenarios 2 and 3 this can be explained by the high response rate of the agents who most likely react to the decline in fitness caused by short-term episodes of overcrowding, rather than actual declines in K.

8.5 Conclusions

This study proposed a model of the emergence and transformation of human settlement pattern by combining a series of assumptions drawn from evolutionary ecology. The two objectives of the simulation exercise were to identify the equilibrium properties of the system in a disturbance-free context (scenario 0), and subsequently explore how four types of perturbations (scenarios 1–4) can affect these. We can summarise the main outcomes of the first objective as follows:

- Convex systems can sustain stable equilibria as long as the level of system connectivity is relatively low;
- Primate systems emerge only temporarily, either as part of a limit-cycle equilibrium, or as a short-term transition from a convex equilibrium. In either case, they require some level of system connectivity, defined here by the spatial range of interaction (h), the frequency of decision-making (z), and the sample proportion of observed neighbour agents (k);
- More generally, increasing connectivity determines an increase in the instability of the system, from a narrowly confined convex point attractor to high frequency oscillations between primate and convex systems, with intermediate states characterised by either point attractors with frequent "escapes" or by more gradual shifts between opposite values of A.

When the system is characterised by low levels of connectivity, individual groups are trapped within local optima while being spatially isolated from each other. Variations in group size will be primarily driven by intrinsic growth rate, as inter-group movement of the agents becomes rare. Interestingly, spatial heterogeneity in the resource distribution (scenario 1) does not affect the dynamics of the system, as agents rapidly find the most suitable locations to settle in the first few runs of the simulation. Once we allow a larger range of interaction, groups become less isolated from each other. This means that small variations in fitness (determined by stochastic components in the model) are amplified by subsequent inter-group migrations. We can conceptualise this with a simple thought experiment. Consider two communities A and B with the same group size. Small differences in the individual yields and random occurrence of reproduction will determine a divergence in their sizes and hence fitness in the short term. Thus, members of A might have a slightly higher fitness than members of B. In the long-term these differences will vanish, but if any individual of B moves to A, this difference will be amplified. Group A will have higher fitness and hence higher chance to further increase its size through reproduction, while members of B will be more attracted by A. If we extend this to a larger number of groups, these dynamics will be further enhanced. As long as the frequency of decision-making is sufficiently high these small variations in the systems will be "detected", and when the spatial range of interaction and the sample proportion of observed agents are both high, chances of agents sharing the same destination becomes increasingly high. This will have a

cascade effect, with the sudden appearance of large nucleated settlements (primate systems). These are however highly unstable, and hence their formation will be followed by fission events, which reset and drive the cyclical behaviour of the system.

The low resilience of primate systems is perhaps counter-intuitive, given that in many real-world contexts we can frequently observe these patterns with some degree of stability over time. We should however note that the model proposed here does not allow any form of innovation, and hence the structural properties of the system (defined by the model parameters) remain fixed. This is not the case in many real-world contexts, where the exploitation of novel resources and the adoption of new technology are often enhanced by higher population density (Powell et al. 2009; Lake and Crema 2012). These innovations can easily modify the shape of the fitness curve, allowing for the ability to overcome the problem of declining fitness for larger groups. Furthermore, warfare and direct competitions of resources between different groups can also help in maintaining large nucleated settlements at the expense of others, further allowing the system to prolong primate rank-size patterns. Nevertheless, other studies have demonstrated how these settlements are still destined to collapse or fission in the long-term (Turchin 2003; Griffin 2011), and even when a hierarchical system conserves its shape at the macro-scale, individual communities might be affected by turn-overs, continuously changing their ranks (Batty 2006).

Disturbance processes have a major role when the system is characterised by intermediate levels of connectedness. However, the most relevant conclusion here is that they act as a catalyst rather than being the fundamental cause of shifts in the rank-size distribution. If the necessary preconditions, such as high frequency of decision-making or large spatial range of interaction, do not exist, the system will be almost identical to the expected behaviour in a disturbance-free context. Instead, when these preconditions are met, we can observe a larger number of sudden changes in the rank-size distribution in the form of strange and limit-cycle attractors. However, when the spatial range of interaction, the frequency of decision-making and the sample proportion of observed agents are all low, convex point attractors are minimally affected. Exceptions to this occur only when the abruptness of changes in K is high (e.g. high values of v in scenario 3), but the system will still tend to revert to high values of A in the long term. Similarly, at the opposite end of the parameter space (i.e. when z, h, and k are all high), the benchmark and the disturbance models are almost identical, with only some minor differences observable for scenario 4. This is explained by high rates of settlement reorganisation that, within these regions of the parameter space, would occur regardless of disturbance events.

These conclusions enable us to build a template to which empirical archaeological data can be compared. The abstract nature of the model does not allow us to have precise predictions on the parameters for specific contexts, but, nonetheless, identifying different proxies on the connectivity of the system could provide some clues on why a given rank-sized distribution emerged or changed over time. Thus, one should expect that a rugged landscape might favour the isolation between different communities compared to a plain region, and quantify such an expectation

using models of movement based on GIS-led analysis (Conolly and Lake 2006; Bevan 2011) or more complex methods based on circuit-scape theory (McRae et al. 2008). Other proxies for evaluating the degree of system integration include the formal assessment of patterns of cultural similarity or dissimilarity between different communities. Both empirical (Lipo et al. 1997; Shennan and Bentley 2008) and theoretical works (Premo and Scholnick 2011; Crema et al. 2014) have shown great potential for these studies for investigating the strength and variations of regional interaction. Bevan and Wilson (2013) provide a recent example on how these assumptions can also be integrated into realistic models of settlement evolution, allowing for the possibility to directly compare observed data with model predictions.

While these research directions are strongly encouraged, it is also crucial that the underpinning theories of these models are dissected first in artificial and abstract environments where we have full control of each variable. We still need to fully examine the consequences of our theoretical assumptions, before proceeding in applying these models to comprehend real-world changes in human settlement pattern. This chapter is a contribution to such an endeavour.

Acknowledgements I would like to thank the editors for inviting me to contribute to this volume and for providing me rapid feedback during all the editorial process. I am extremely grateful to Andrew Bevan and Mark Lake for discussions and constructive critiques on virtually every aspect of the manuscript and to the two anonymous reviewers for providing valuable comments. This research was funded by a UCL Graduate School Research Scholarship and the AHRC Centre for the Evolution of Cultural Diversity, and acknowledges the use of the UCL *Legion* High Performance Computing Facility (Legion@UCL) and associated support services.

References

Allee WC (1951) The Social Life of Animals. Beacon Press, Boston

Batty M (2006) Rank clocks. Nature 444:592–596

Bevan A (2011) Computational Models for Understanding Movement and Territory. In: Herrera VM, Pérez SC (eds) Tecnologías de Información Geográfica y Análisis Arqueológico del Territorio, Anejos de Archivo Español de Arqueología, Mérida, pp 383–394

Bevan A, Wilson A (2013) Models of settlement hierarchy based on partial evidence. J Archaeol Sci 40(5):2415–2427

Clark CW, Mangel M (1986) The evolutionary advantages of group foraging. Theor Popul Biol 30:45–75

Conolly J, Lake M (2006) Geographical Information Systems in Archaeology. Cambridge University Press, Cambridge

Crema ER (2013a) Cycles of change in Jomon settlement: a case study from eastern Tokyo bay. Antiquity 87(338):1169–1181

Crema ER (2014) A simulation model of fission-fusion dynamics and long-term settlement change. J Archaeol Method Theory 21, 385–404

Crema ER (2013b) Spatial and Temporal Models of Jomon Settlement. Ph.D. thesis, University College London, unpublished

Crema ER, Kerig T, Shennan S (2014) Culture, space, and metapopulation: a simulation-based study for evaluating signals of blending and branching. J Archaeol Sci 43, 289–298

Drennan RD, Peterson CE (2004) Comparing archaeological settlement systems with rank-size graphs: a measure of shape and statistical confidence. J Archaeol Sci 31(5):533–549
Drucker P (1951) The Northern and Central Nootkan Tribes. Smithsonian Institution Bureau of American Ethnology, Washington, Bulletin 144
Endo M (1995) The mobility of resident members of the Ainu in Hokkaido, Japan, in the mid-nineteenth century. Sci Rep Tohoku Univ Ser 7 45(2):75–102
Fagen R (1987) A generalized habitat matching rule. Evol Ecol 1:5–10
Fortin MJ, Dale M (2005) Spatial Analysis: A Guide for Ecologists. Cambridge University Press, Cambridge
Fretwell SD, Lucas HL (1970) On territorial behavior and other factors influencing habitat distribution in birds. I. Theoretical development. Acta Biotheor 19:16–36
Giraldeau LA, Caraco T (2000) Social Foraging Theory. Princeton University Press, Princeton
Gould RA, Yellen JE (1987) Man the hunted: determinants of household spacing in desert and tropical foraging societies. J Anthropol Archaeol 6:77–103
Greene CM, Stamps JA (2001) Habitat selection at low population densities. Ecology 82: 2091–2100
Griffin AF (2011) Emergence of fusion/fission cycling and self-organized criticality from a simulation model of early complex polities. J Archaeol Sci 38:873–883
Hawkes K (1992) Sharing and Collective Action. In: Smith EA, Winterhalder B (eds) Evolutionary Ecology and Human Behaviour. Aldine de Gruyter, New York, pp 269–300
Henrich J (2001) Cultural transmission and the diffusion of innovations: adoption dynamics indicate that biased cultural transmission is the predominate force in behavioral change. Am Anthropol 103(4):992–1013
Hodder I (1979) Simulating the Growth of Hierarchies. In: Renfrew C, Cooke KL (eds) Transformtaions: Mathemathical Approaches to Culture Change. Academic, New York, pp 117–144
Johnson GA (1980) Rank-size convexity and system integration: a view from archaeology. Econ Geogr 56:234–247
Jones R (2010) The village and the butterfly: nucleation out of chaos and complexity. Landscapes 1:25–46
Kennett D, Anderson A, Winterhalder B (2006) The Ideal Free Distribution, Food Production, and the Colonization of Oceania. In: Kennett DJ, Winterhalder B (eds) Behavioral Ecology and the Transition to Agriculture. University of California Press, Berkeley, pp 265–288
Kohler TA, Varien MD (2010) A Scale Model of Seven Hundred Years of Farming Settlements in Southwestern Colorado. In: Bandy MS, Fox KR (eds) Becoming Villagers: Comparing Early Village Societies. University of Arizona Press, Tucson, pp 37–61
Lake MW, Crema ER (2012) The cultural evolution of adaptive-trait diversity when resources are uncertain and finite. Adv Complex Syst 15(1 & 2):1150013. DOI 10.1142/S0219525911003323. http://dx.doi.org/10.1142/S0219525911003323
Lipo CP, Madsen ME, Dunnell RC, Hunt T (1997) Population structure, cultural transmission, and frequency seriation. J Anthropol Archaeol 16:301–333
McGlade J (1995) Archaeology and the ecodynamics of human-modified landscapes. Antiquity 69:113–132
McRae BH, Dickson BG, Keitt TH, Shah VB (2008) Using circuit theory to model connectivity in ecology, evolution, and conservation. Ecology 89:2712–2724
Mithen SJ (1990) Thoughtful Foragers: A Study of Prehistoric Decision Making. Cambridge University Press, Cambridge
Pelletier DL, Frongillo EA, Habicht JP (1993) Epidemiologic evidence for a potentiating effect of malnutrition on child mortality. Am J Public Health 83(8):1130–1133
Powell A, Shennan S, Thomas MG (2009) Late Pleistocene demography and the appearance of modern human behavior. Science 324:1298–1301
Premo LS (2010) Equifinality and Explanation: The Role of Agent-Based Modeling in Postpositivist Archaeology. In: Costopoulos A, Lake M (eds) Simulating Change: Archaeology into the Twenty-First Century. University of Utah Press, Salt Lake City, pp 28–37

Premo LS, Scholnick JB (2011) The spatial scale of social learning affects cultural diversity. Am Antiq 76(1):163–176. http://saa.metapress.com/index/A661T246K0J1227K.pdf
R Core Team (2013) R: A Language and Environment for Statistical Computing. R Foundation for Statistical Computing. Software. http://www.R-project.org
Roberts BK (1996) Landscapes of Settlement: Prehistory to the Present. Routledge, London
Savage SH (1997) Assessing departures from log-normality in the rank-size rule. J Archaeol Sci 24:233–244
Shennan SJ, Bentley AM (2008) Interaction, and Demography Among the Earliest Farmers of Central Europe. In: O'Brien MJ (ed) Cultural Transmission and Archaeology: Issues and Case Studies. SAA Press, Washington, pp 164–177
Sibly RM (1983) Optimal group size is unstable. Anim Behav 31(3):947–948
Sutherland WJ (1983) Aggregation and the "ideal free" distribution. J Anim Ecol 52:821–828
Tregenza T (1995) Building on the ideal free distribution. Adv Ecol Res 26:253–302
Turchin P (2003) Historical Dynamics: Why States Rise and Fall. Princeton University Press, Princeton
Verhulst PF (1838) Notice sur la loi que la population poursuit dans son accroissement. Correspondance Math. Phys. 10:112–121
Watanabe H (1986) Community Habitation and Food Gathering in Prehistoric Japan: An Ethnographic Interpretation of the Archaeological Evidence. In: Pearson RJ, Barnes GL, Hutterer KL (eds) Windows on the Japanese Past: Studies in Archaeology and Prehistory. Centre for Japanese Studies, University of Michigan, Ann Arbor, pp 229–254
Winterhalder B, Kennett DJ, Grote MN, Bartruff J (2010) Ideal free settlement of California's Northern Channel Islands. J Anthropol Archaeol 29:469–490
Zipf GK (1949) Human Behavior and the Principle of Least Effort. Harvard University Press, Cambridge